Senoue, column 1, line 33 *et seq*. Further, the Examiner alleges that the gases disclosed as being in a CVD chamber citing Senoue, column 4, line 53 *et seq*.

The claimed invention as amended is drawn to a chamber cleaning gas for treating a plasma CVD chamber with at least one of the claimed carbon fluorocarbons to remove byproducts formed on the CVD chamber. For exemplary purposes only, such byproducts include silicon, polysilicon, tungsten, titanium and their oxides, nitrites and carbides (see specification, page 2, line 23 - page 3, line 1). Further, the claimed cleaning method may be used to remove any byproduct formed on a CVD chamber which one of ordinary skill in the art would expect to be formed on the inside of a CVD chamber resulting during CVD processing.

The present invention is not anticipated by Senoue as Senoue fails to teach or suggest a chamber cleaning gas comprising the claimed gases. Therefore, the chamber gas must have the physical and chemical characteristics necessary for plasma CVD chamber cleaning.

Contrary to the Examiner's assertion, Senoue fails to teach or suggest a plasma CVD chamber cleaning gas. On the contrary, Senoue is completely silent as to a CVD chamber cleaning gas. Senoue is specifically directed to removing an etching residue or polymer from a substrate or a semiconductor material but clearly not a chamber wall. Moreover, Senoue fails to teach or suggest let alone motivate one of ordinary skill in the art to use its <u>etching gas</u> on the walls of a CVD chamber.

Evidence of these uses is provided in Senoue, which discloses treatment to remove the etching residue or polymer, or to inhibit the corrosion of the semiconductor material (Senoue, column 1, lines 64-66). Further, Senoue teaches the etching of silicon by a fluorohydrocarbon gas such as tetrafluoromethane which relates to

fluorocarbon polymer deposits on a silicon surface (Senoue, column 2, lines 26-29). In addition, the polymer residue to be etched is one that remains on the silicon oxide material, i.e., the silicon semiconductor substrate (Senoue, column 2, lines 31-32).

Further evidence that the Senoue gases are used to clean a silicon substrate rather than for use in cleaning a CVD wall is provided in Senoue which clearly discloses that no contamination was observed on the surface of the substrate (Senoue, column 5, lines 20-21); no roughening or contamination was observed on the silicon substrate surface (Senoue, column 5, lines 36-37); no formation of any polymer was observed on the substrate surface (Senoue, column 5, lines 48-50); and a cleaning treatment of a semiconductor material is provided using the disclosed gas(es) (Senoue, column 6, lines 6-7).

In sharp contrast to Senoue, the present invention relates to a cleaning gas which can easily and effectively remove reactant byproducts attached to the CVD chamber walls (see the present specification, page 2, lines 20-22).

Contrary to the Examiner's allegation that the application of the gases in Senoue is used in a CVD chamber citing Senoue, column 4, line 53 *et seq.*, the cited section discloses that the etching treatment of the polysilicon layer was conducted while C_3F_6O and Cl_2 gases were introduced into the etching chamber. Thus, the Senoue's gases are used in an etching chamber, not a CVD chamber. Therefore, contrary to the Examiner's allegation, Senoue clearly teaches the use of its gases in an etching chamber and not a CVD chamber.

Furthermore, due to the differences in byproducts formed on an etching chamber wall versus a CVD chamber wall, there fails to be any teaching let alone any suggestion or motivation for one of ordinary skill in the art to use the gases of Senoue in a CVD

chamber. The differences in byproducts formed on an etching chamber wall and a CVD chamber wall is due to the fact that etching and CVD are different procedures.

In etching using a fluorocarbon gas, for example, fluorocarbon polymers will be deposited on the etching chamber walls. Those fluorocarbon polymers are removed mainly by oxygen plasma after the etching process.

On the other hand, in CVD which deposits SiO_2, SiN, etc., on a wafer surface, for example, some SiO_2, SiN, etc., will be deposited on CVD chamber walls. Those byproducts are removed by fluorine radicals (•F) generated from a cleaning gas, such as NF_3 or fluorocarbon gases together with oxygen. It should be noted that oxygen is required when using fluorocarbon gases for cleaning, as fluorocarbon polymers derived from fluorocarbon gases will be deposited on the chamber walls to some extent.

In the present invention, it was determined that hexafluoropropylene oxide and hexafluoroacetone are efficient cleaning gases for plasma CVD chambers, not only because they generate fluorine radicals, but also they have oxygen atom themselves.

Moreover, Applicant wishes to re-emphasize and reiterate the differences between cleaning gases and etching gases.

Etching gases and cleaning gases are not interchangeable. A gas, working preferably as an etching gas, is irrelevant to a preferable cleaning gas. This is because the properties required for a cleaning gas and an etching gas are different due to their roles as previously mentioned and described in the Remarks section to the Amendment filed on March 11, 2002.

In short, a cleaning gas can just remove all byproducts formed on the chamber walls. However, an etching gas is required to have a high selectivity between what is

etched and what is not etched, and a high aspect ratio. Accordingly, it is natural that a suitable cleaning gas and a suitable etching gas should be different.

Moreover, CVD chamber devices and etching chamber devices are distinctive devices. Evidence of this is provided by the attached Reference A, which shows separate plasma etching chambers and CVD systems and/or processing chambers. Accordingly, an etching gas is not suitable for a cleaning gas because an isotropic etching or a cleaning in a certain direction is thus not suitable for cleaning.

Furthermore, Senoue fails to teach or even suggest a method of cleaning a CVD chamber let alone using the claimed gases as recited in claims 15, 16 and 18 in a CVD chamber cleaning method.

Based on the foregoing discussion, Applicant respectfully submits that claims 11, 12, 14-16 and 18 are not anticipated by Senoue.

Claims 13 and 17 were rejected under 35 U.S.C. § 102(b) as being unpatentable over Senoue in view of U.S. Patent 4,260,649 to Denison et al (hereinafter "Denison"). The Examiner alleges that every limitation of claims 13 and 17 is disclosed in Senoue except that Senoue fails to explicitly disclose a gas of hexafluoroacetone and its use as an etchant. However, the Examiner states "it is believed to be subsumed within the fluoro gas and process gases alluded to in Senoue". In addition, the Examiner points to Denison in alleging the missing element.

The Examiner mentions that Examples VI discloses that a hexafluoroacetone gas, used in conjunction with oxygen may be used to strip photoresist, and that thus Denison "teaches using the chemical of claim 17 for the purpose of claim 17 (i.e., removal of unwanted material from the plasma CVD chamber)."

Contrary to the Examiner's allegation, Denison does not teach the use of a hexafluoroacetone gas in conjunction with oxygen to strip a photoresist.

To be precise, Denison discloses that hexafluoroacetone can be used instead of CF_3I in Example I (column 4, lines 38-42; please note that this paragraph is not included in Example VI). In other words, Denison discloses that selective etching of a silicon oxide layer overlaying a silicon wafer substrate workpiece is obtained by hexafluoroacetone.

Accordingly, Denison does not mention that hexafluoroacetone is used to strip photoresist.

Therefore, Applicant respectfully submits that the Examiner's assertion is incorrect. Thus, Applicant respectfully submits that claims 13 and 17 are not obvious from Senoue individually or in combination with Denison.

In view of the foregoing, Applicant respectfully submits that the present application is in condition for allowance.

Respectfully submitted,

LARSON & TAYLOR, PLC

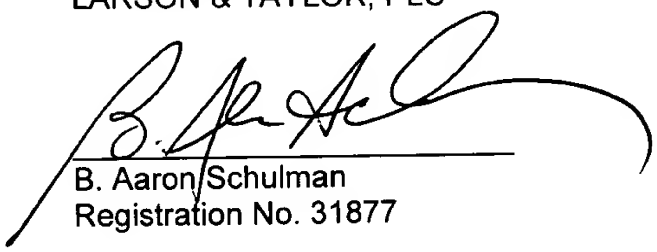

B. Aaron Schulman
Registration No. 31877

1199 North Fairfax Street, Suite 900
Alexandria, Virginia 22314
(703) 739-4900

February 21, 2003

ATTACHMENT A

Marked Up Replacement Claims

Following herewith is a marked up copy of rewritten claim 11, together with all other pending claims.

11. (Amended) A chamber cleaning gas for plasma CVD chambers comprising at least one gas selected from the group consisting of 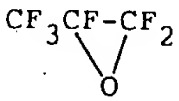 and 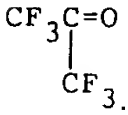 .

12. A chamber cleaning gas according to claim 11 comprising hexafluoropropylene oxide represented by the formula 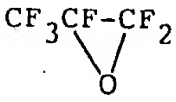 .

13. A chamber cleaning gas according to claim 11 comprising CF_3COCF_3.

14. A chamber cleaning gas according to claim 11 which further comprises at least one monomer gas selected from the group consisting of He, Ne, Ar, H_2, N_2 and O_2.

15. A chamber cleaning method comprising the step of treating a plasma CVD chamber of a semiconductor integrated circuit production device with at least one chamber cleaning gas selected from the group consisting of 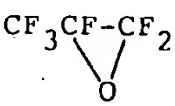 and 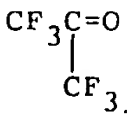 .

16. A chamber cleaning method according to claim 15 wherein the chamber cleaning gas is hexafluoropropylene oxide represented by the formula 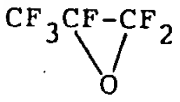 .

17. A chamber cleaning method according to claim 15 wherein the chamber cleaning gas is CF_3COCF_3.

18. A chamber cleaning method according to claim 15 which further comprises at least one monomer gas selected from the group consisting of He, Ne, Ar, H_2, N_2 and O_2.

ATTACHMENT B

Clean Replacement (Entire Set Of Pending Claims)

Following herewith is a clean copy of the entire set of pending claims.

11. (Amended) A chamber cleaning gas for plasma CVD chambers comprising at least one gas selected from the group consisting of 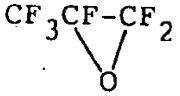 and 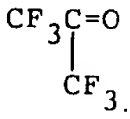 .

12. A chamber cleaning gas according to claim 11 comprising hexafluoropropylene oxide represented by the formula 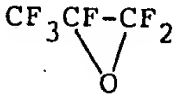 .

13. A chamber cleaning gas according to claim 11 comprising CF_3COCF_3.

14. A chamber cleaning gas according to claim 11 which further comprises at least one monomer gas selected from the group consisting of He, Ne, Ar, H_2, N_2 and O_2.

15. A chamber cleaning method comprising the step of treating a plasma CVD chamber of a semiconductor integrated circuit production device with at least one chamber cleaning gas selected from the group consisting of 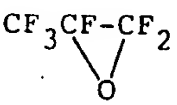 and 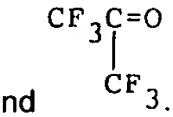 .

16. A chamber cleaning method according to claim 15 wherein the chamber cleaning gas is hexafluoropropylene oxide represented by the formula 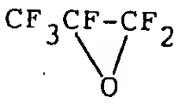 .

17. A chamber cleaning method according to claim 15 wherein the chamber cleaning gas is CF_3COCF_3.

18. A chamber cleaning method according to claim 15 which further comprises at least one monomer gas selected from the group consisting of He, Ne, Ar, H_2, N_2 and O_2.

Reference A

Highlights

Venue: Pacifico Yokohama
Exhibition Hall

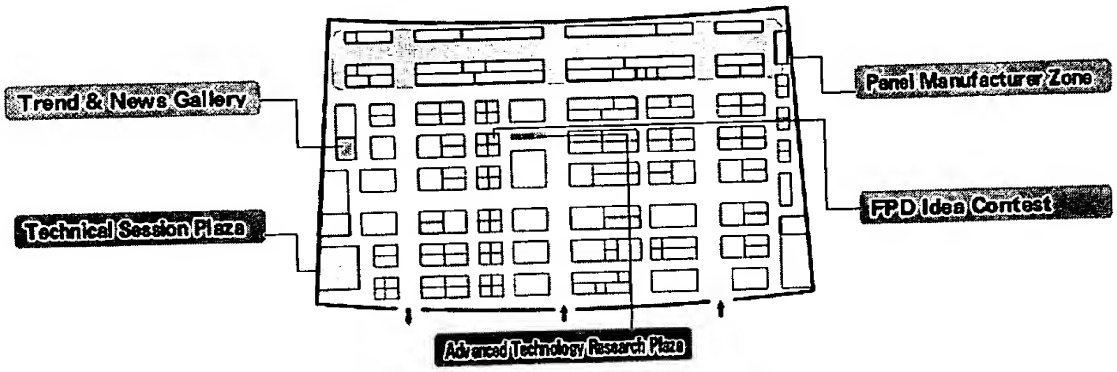

Exhibit Products

Substrate Process Related
Glass substrate polishing and coating equipment, exposure equipment, resist coater/ developer, etching equipment (wet/ dry), CVD device, sputtering apparatus, cleaning system, ion doping system, laser annealing system, etc.

LCD Cell/ Module Assembly Related
Cleaning equipment, orientation film coating equipment, rubbing equipment, calcination equipment, screen printer, spacer dispersion equipment, pasting equipment, pressure adhesive/ hardening equipment, liquid crystal injection equipment, sealing equipment, cell separation equipment, TAB mounting equipment, deflector plate attaching equipment, others.

Manufacturing Equipment for PDP
Vacuum vapor depositing equipment, sputtering equipment, exposure equipment, etching equipment, asher, screen printer, sand blasting equipment, calcination furnace, glass separation equipment, assembly positioning equipment, glass chamfering equipment, mounting furnace, exhaust, gas injection equipment, driver mounting equipment, washing-wet treatment equipment, aging equipment, others.

Parts and Materials
Glass/ plastic substrate, Glass substrate with ITO film, color filter, resist, developing fluid, photo mask, screen mask, driver controller LSI, gas, orientation film, liquid crystal material, spacer material, deflection plate, phase differential plate, light guiding plate, diffusion plate, light collection sheet, vision angle expansion film, back light unit, lamp, anisotropic conductive film, metal material target, protective film target, dielectric target, insulator target, dry film for sandblasting, shield film, conductive paste, insulating paste, fluorescent material, sandblasting material, sealing material, others

Inspection, Measuring and Repairing Equipment
Glass substrate inspection equipment, lamp inspection equipment, array inspection equipment, film pressure/ resistance measuring instrument, prober, environment test equipment, repair equipment, others

Related Facilities, Equipment and Parts
Transporting equipment, clean room, electrostatic remedied products, air conditioner/ gas related, cleaning/ chemical solution related, piping, valve, filter, pump, mass flow controller, cassette carrier, production control system, process control system, others

Designing, Manufacturing Support Software
Simulation software, CAD software, EDA tool, quality control system, process control system, others

Clean room Related Products/ Equipment

Liquid Crystal Display/ Module
TFT, STN, TN and other liquid crystal display/ module, liquid crystal projector, others

Plasma Display Panel

Organic EL Related
Organic thin film material, electrode material, sealing material, phosphor, color filter, film generating equipment, display panel module.

Other Flat Panel Displays
Micro display, inorganic EL, DMD, FED, LED, others

Imaging Devices
Various ASSP, including image compression/ expansion LSI, various boards

Display applied products

Newspaper, publication, survey

STANDARD EQUIPMENT INDEX

PROCESS SYSTEMS

DRIE–1000 SERIES SYSTEMS: *SINGLE CHAMBER PLASMA PROCESSING.*

DRIE–1200–LL–ICP (*NEW !!*): HIGH DENSITY PLASMA ETCHER FOR ANISOTROPIC APPLICATIONS. 200mm WAFER CAPABILITIES.

MPS–2000 SERIES SYSTEMS: *INLINE MULTI–CHAMBER PLASMA PROCESSING.*

PDS–6000 CLUSTER TOOL: *PRODUCTION SYSTEM WITH CENTRAL DISTRIBUTION LOADLOCK & ROBOT.*

DRIE–1100–LL–ECR: *DRIE SERIES HIGH–DENSITY PLASMA SYSTEMS WITH ELECTRON CYCLOTRON RESONANCE SOURCE.*

UHV–CVD–5000: *ULTRA–HIGH VACUUM CHEMICAL VAPOR DEPOSITION.*

VES–3000 BELL–JAR COATERS: *VACUUM EVAPORATION / METALLIZATION. THERMAL, E–BEAM, & SPUTTERING.*

CVD–300 SYSTEM: *THERMAL CVD VACUUM FURNACE IDEAL FOR RESEARCH AND SMALL–SCALE PRODUCTION.*

PECVD–60 SYSTEM: *R&D MICROWAVE PLASMA CVD. DIAMOND, BORON NITRIDE, SILICON CARBIDE, ETC.*

LPE–4750 SYSTEM: *PRODUCTION LIQUID–PHASE EPITAXY. GaAs, GaP, InP, ETC.*

MSI–3000 SYSTEM: *A COMPLETE MASS SPECTROMETER GAS HANDLING AND INLET TOOL FOR GAS CONTROL AND NUCLEAR SERVICE APPLICATIONS.*

LRGAS–100, –200, –300: *RGA GAS ANALYSIS SYSTEMS MOUNTED IN A MOBILE CART. COMPLETE WITH 100, 200, OR 300 AMU RGA HEAD, TURBO PUMP SYSTEM, VACUUM GAUGING, COMPUTER, AND CONTROL PANEL. DRY (OIL FREE) CONFIGURATIONS AVAILABLE.*

MOCVD 500–A: *AN R&D METAL–ORGANIC CVD SYSTEM.*

MBE–6000 SYSTEM: *R&D MOLECULAR BEAM EPITAXY.*

PA–3000–A ETCHER: *A BATCH PLASMA ASHING MODULE. APPLICATIONS FOR CLEANING WAFERS, PC BOARD DESMEARING, AND REACTIVE ION ETCH. PROCESS UP TO 200 SILICON WAFERS PER LOAD.*

GENERAL PURPOSE EQUIPMENT

VACUUM CHAMBERS: *ALTITUDE TESTING, DEGASSING, INERT GAS STORAGE, IMPREGNATION, ETC.*

GLOVEBOXES: *PROVIDES INERT ENVIRONMENT FOR HANDLING & STORING REACTIVE MATERIALS.*

ACCESSORIES

BURNBOX / SCRUBBER MODULES: *TREATMENT OF COMMON SEMICONDUCTOR PROCESS EXHAUST GASES.*

VARI–VAC ® GAS METERING VALVES: *A LOW COST METHOD OF DELIVERING PRECISION GAS FLOW.*

PHOTORESIST CURING SYSTEM: *THERMAL BAKE OUT PROCESSING FOR SUBSTRATE SIZES TO 12" X 12" SQUARE.*

GAS DISTRIBUTION: *TEK–VAC OFFERS VARIOUS ENGINEERING, DESIGN, AND MANUFACTURING SERVICES FOR EQUIPMENT SUB–ASSEMBLIES.*

FLO–MASTER FM–2001: *A POWER SUPPLY, FLOW CONTROL, AND FLOW READOUT DEVICE, INTENDED TO CONTROL MOST COMMERCIALLY*

AVAILABLE MASS FLOW CONTROLLERS.

ION GAUGE TUBES: *STANDARD BAYARD–ALPERT IONIZATION GAUGE TUBE WITH YOUR CHOICE OF FITTINGS (TUBULATION, CONFLAT, KF–25).*

PRINCIPLES OF PLASMA DISCHARGES AND MATERIALS PROCESSING

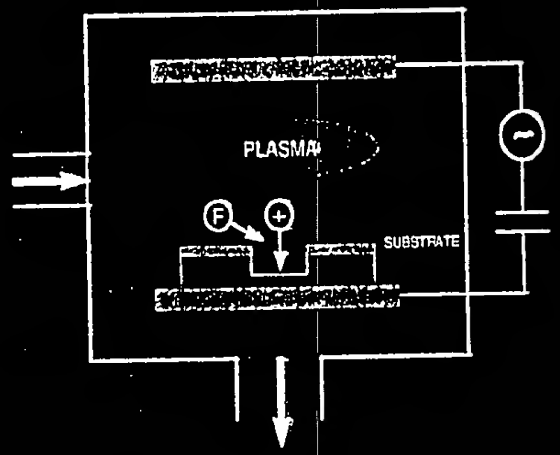

MICHAEL A. LIEBERMAN
ALLAN J. LICHTENBERG

Timely, authoritative, pedagogically consistent—a valuable professional resource and a superior didactic tool.

Authored by two internationally respected pioneers in the field, this book offers a fully integrated, pedagogically consistent presentation of the fundamental physics and chemistry of partially ionized, chemically reactive, low-pressure plasmas and their roles in a wide range of plasma discharges and processes used in thin film processing applications—especially in the fabrication of integrated circuits. With many fully worked examples, practice exercises, and clear demonstrations of the relationship of plasma parameters to external control parameters and processing results, this book combines the best qualities of a student text and a professional resource.

- In-depth coverage of the fundamentals of plasma physics and chemistry—includes separate chapters on atomic and molecular collisions
- Applies basic theory to plasma discharges, including calculations of plasma parameters and scaling of plasma parameters with control parameters
- Applies results to basic processing mechanisms and the effects of plasma parameters on those mechanisms
- Uses numerous worked examples to demonstrate the relationships between control parameters, plasma parameters, and processing results

MICHAEL A. LIEBERMAN, PhD, is Professor of Electrical Engineering at the University of California, Berkeley, and Director of the Berkeley Electronics Research Laboratory. He has published more than 140 journal articles on the topics of plasmas, plasma processing, and nonlinear dynamics. He has also published, with Professor Lichtenberg, *Regular and Stochastic Motion* and *Regular and Chaotic Dynamics, Second Edition*.

ALLAN J. LICHTENBERG, PhD, is Professor of Electrical Engineering at the University of California, Berkeley. A respected pioneer in the fields of high-temperature plasmas, plasma discharges, and nonlinear dynamics, Dr. Lichtenberg has written over 100 articles in these areas. In addition to the books coauthored with Professor Lieberman, he has written an earlier monograph *Phase Space Dynamics of Particles*.

Cover Design: David Levy

WILEY-INTERSCIENCE
John Wiley & Sons, Inc.
Professional, Reference and Trade Group
605 Third Avenue, New York, N.Y. 10158-0012
New York • Chichester • Brisbane • Toronto • Singapore

Practical Formulae

In the following practical formulae, n_e is in units of cm^{-3}, T_e is in volts, and B is in gauss (1 tesla = 10^4 gauss).

Electron plasma frequency	$\omega_{pe} = (e^2 n_e/\epsilon_0 m)^{1/2}$	$f_{pe} = 9000\sqrt{n_e}$ Hz
Electron gyration frequency	$\omega_{ce} = eB/m$	$f_{ce} = 2.8B$ MHz
Electron Debye length	$\lambda_{De} = (\epsilon_0 T_e/en_e)^{1/2}$	$\lambda_{De} = 740\sqrt{T_e/n_e}$ cm
Mean electron speed	$\bar{v}_e = (8eT_e/\pi m)^{1/2}$	$\bar{v}_e = 6.7 \times 10^7\sqrt{T_e}$ cm/s
Bohm velocity	$u_B = (eT_e/M)^{1/2}$	$u_B = 9.8 \times 10^5\sqrt{T_e/A_R}$ cm/s

CHAPTER 1

INTRODUCTION

1.1 MATERIALS PROCESSING

Chemically reactive plasma discharges are widely used to modify the surface properties of materials. Plasma processing technology is vitally important to several of the largest manufacturing industries in the world. Plasma-based surface processes are indispensable for manufacturing the very large scale integrated circuits (ICs) used by the electronics industry. Such processes are also critical for the aerospace, automotive, steel, biomedical, and toxic waste management industries. Materials and surface structures can be fabricated that are not attainable by any other commercial method, and the surface properties of materials can be modified in unique ways. For example, 0.2-μm-wide, 4-μm-deep trenches can be etched into silicon films or substrates (Fig. 1.1). A human hair is 50–100 μm in diameter, so hundreds of these trenches would fit endwise within a human hair. Unique materials such as diamond films and amorphous silicon for solar cells have also been produced, and plasma-based hardening of surgically implanted hip joints and machine tools have extended their working lifetimes manyfold.

It is instructive to look closer at integrated circuit fabrication, which is the key application that we describe in this book. As a very incomplete list of plasma processes, argon or oxygen discharges are used to sputter-deposit aluminum, tungsten, or high-temperature superconducting films; oxygen discharges can be used to grow SiO_2 films on silicon; SiH_2Cl_2/NH_3 and $Si(OC_2H_5)_4/O_2$ discharges are used for the

FIGURE 1.1. Trench etch (0.2 μm wide by 4 μm deep) in single-crystal silicon, showing the extraordinary capabilities of plasma processing; such trenches are used for device isolation and charge storage capacitors in integrated circuits.

plasma-enhanced chemical vapor deposition of Si_3N_4 and SiO_2 films, respectively; BF_3 discharges can be used to implant dopant (B) atoms into silicon; $CF_4/Cl_2/O_2$ discharges are used to selectively remove silicon films; and oxygen discharges are used to remove photoresist or polymer films. These types of steps (deposit or grow, dope or modify, etch or remove) are repeated again and again in the manufacture of a modern integrated circuit. They are the equivalent, on a micrometer-size scale, of centimeter-size manufacture using metal and components, bolts and solder, and drill press and lathe. For microfabrication of an IC, one-third of the tens to hundreds of fabrication steps are typically plasma-based.

Figure 1.2 shows a typical set of steps to create a metal film patterned with submicrometer features on a large area (200-mm-diameter) wafer substrate. In (a), the film is deposited; in (b), a photoresist layer is deposited over the film; in (c), the resist is selectively exposed to light through a pattern; and in (d), the resist is developed, removing the exposed resist regions and leaving behind a patterned resist mask. In (e), this pattern is transferred into the film by an etch process; the mask protects the underlying film from being etched. In (f), the remaining resist mask is removed. Of these six steps, plasma processing is generally used for film deposition (a) and etch (e), and may also be used for resist development (d) and removal (f).

The etch process in (e) is illustrated as leading to vertical sidewalls aligned with the resist mask; i.e, the mask pattern has been faithfully transferred into the metal film. This can be accomplished by an etch process that removes material in the vertical direction only. The horizontal etch rate is zero. Such *anisotropic* etches are easily produced by plasma processing. On the other hand, one might imagine

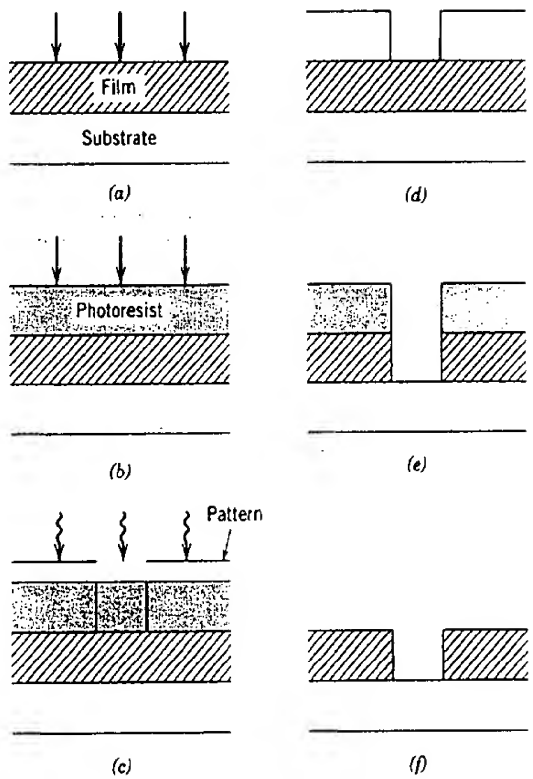

FIGURE 1.2. Deposition and pattern transfer in manufacturing an integrated circuit: (a) metal deposition; (b) photoresist deposition; (c) optical exposure through a pattern; (d) photoresist development; (e) anisotropic plasma etch; (f) remaining photoresist removal.

that exposing the masked film (d) to a liquid (or vapor phase) etchant will lead to the undercut *isotropic* profile shown in Fig. 1.3a (compare to Fig. 1.2e), which is produced by equal vertical and horizontal etch rates. Many years ago, feature spacings (e.g., between trenches) were tens of micrometers, much exceeding required film thicknesses. Undercutting was then acceptable. This is no longer true with submicrometer feature spacings. The reduction in feature sizes and spacings makes anisotropic etch processes essential. In fact, strictly vertical etches are sometimes not desired; one wants controlled sidewall angles. Plasma processing is the only commercial technology capable of such control. Anisotropy is a critical process parameter in IC manufacture and has been a major force in driving the development of plasma processing technology.

The etch process applied to remove the film in Fig. 1.2d is shown in Fig. 1.2e as not removing either the photoresist or the underlying substrate. This *selectivity* is another critical process parameter for IC manufacture. Whereas wet etches have been developed having essentially infinite selectivity, highly selective plasma etch

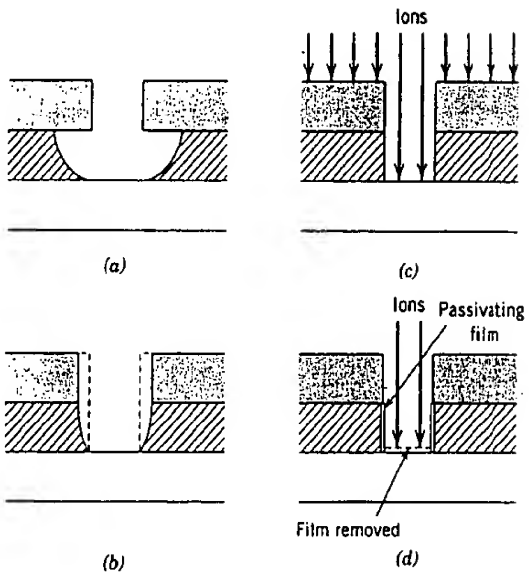

FIGURE 1.3. Plasma etching in integrated circuit manufacture: (a) example of isotropic etch; (b) sidewall etching of the resist mask leads to a loss of anisotropy in film etch; (c) illustrating the role of bombarding ions in anisotropic etch; (d) illustrating the role of sidewall passivating films in anisotropic etch.

processes are not easily designed. Selectivity and anisotropy often compete in the design of a plasma etch process, with results as shown in Fig. 1.3b. Compare this to the idealized result shown in Fig. 1.2e. Assuming that film-to-substrate selectivity is a critical issue, one might imagine simply turning off the plasma after the film has been etched through. This requires a good endpoint detection system. Even then, variations in film thickness and etch rate across the area of the wafer imply that the etch cannot be stopped at the right moment everywhere. Hence, depending on the process *uniformity*, there is a need for some selectivity. These issues are considered further in Chapter 15.

Here is a simple recipe for etching silicon using a plasma discharge. Start with an inert molecular gas, such as CF_4. Excite the discharge to sustain a plasma by electron–neutral dissociative ionization,

$$e + CF_4 \rightarrow 2e + CF_3^+ + F$$

and to create reactive species by electron–neutral dissociation,

$$\begin{aligned} e + CF_4 &\rightarrow e + F + CF_3 \\ &\rightarrow e + 2F + CF_2 \end{aligned}$$

The etchant F atoms react with the silicon substrate, yielding the volatile etch product SiF_4:

$$Si(s) + 4F(g) \rightarrow SiF_4(g)$$

Here, s and g indicate solid and gaseous forms, respectively. Finally, the product is pumped away. It is important that CF_4 does not react with silicon, and that the etch product SiF_4 is volatile, so that it can be removed. This process etches silicon isotropically. For an anisotropic etch, there must be high-energy ion (CF_3^+) bombardment of the substrate. As illustrated in Figs. 1.3c and d, energetic ions leaving the discharge during the etch bombard the bottom of the trench but do not bombard the sidewalls, leading to anisotropic etching by one of two mechanisms. Either the ion bombardment increases the reaction rate at the surface (Fig. 1.3c), or it exposes the surface to the etchant by removing passivating films that cover the surface (Fig. 1.3d).

Similarly, Cl and Br atoms created by dissociation in a discharge are good etchants for silicon, F atoms and CF_2 molecules for SiO_2, O atoms for photoresist, and Cl atoms for aluminum. In all cases, a volatile etch product is formed. However, F atoms do not etch aluminum, and there is no known etchant for copper, because the etch products are not volatile at reasonable substrate temperatures.

We see the importance of the basic physics and chemistry topics treated in this book: (1) plasma physics (Chapters 2 and 4–6), to determine the electron and ion densities, temperatures, and ion bombardment energies and fluxes for a given discharge configuration; and (2) gas-phase chemistry and (3) surface physics and chemistry (Chapters 7 and 9), to determine the etchant densities and fluxes and the etch rates with and without ion bombardment. The data base for these fields of science is provided by (4) atomic and molecular physics, which we discuss in Chapters 3 and 8. We also discuss applications of equilibrium thermodynamics (Chapter 7) to plasma processing. The measurement and experimental control of plasma and chemical properties in reactive discharges is itself a vast subject. We provide brief introductions to some simple plasma diagnostic techniques throughout the text.

We have motivated the study of the fundamentals of plasma processing by examining anisotropic etches for IC manufacture. Other characteristics motivate its use for deposition, surface modification, and isotropic etch requirements. For example, a central feature of the *low-pressure* processing discharges that we consider in this book is that the plasma itself, as well as the plasma–substrate system, is not in thermal equilibrium. This enables substrate temperatures to be relatively low, compared to those required in conventional thermal processes, while maintaining adequate deposition or etch rates. Putting it another way, plasma processing rates are greatly enhanced over thermal processing rates at the same substrate temperature. For example, Si_3N_4 films can be deposited over aluminum films by plasma-enhanced chemical vapor deposition (PECVD), whereas adequate deposition rates cannot be achieved by conventional chemical vapor deposition (CVD) without melting the aluminum film. Chapter 16 gives further details.

The nonequilibrium nature of plasma processing has been known for many years, as illustrated by the laboratory data in Fig. 1.4. In time sequence, this shows first, the

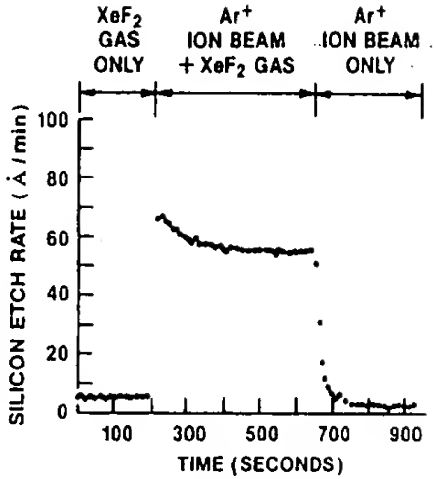

FIGURE 1.4. Experimental demonstration of ion-enhanced plasma etching. (Coburn and Winters, 1979).

equilibrium chemical etch rate of silicon in the XeF_2 etchant gas; next, the tenfold increase in etch rate with the addition of argon ion bombardment of the substrate, simulating plasma-assisted etching; and finally, the very low "etch rate" due to the physical sputtering of silicon by the ion bombardment alone.

A more recent application is the use of plasma-immersion ion implantation (PIII) to implant ions into materials at dose rates that are tens to hundreds of times larger than those achievable with conventional (beam-based) ion implantation systems. In PIII, a series of negative high-voltage pulses are applied to a substrate that is immersed directly into a discharge, thus accelerating plasma ions into the substrate. The development of PIII has opened a new implantation regime characterized by very high dose rates, even at very low energies, and by the capability to implant both large area and irregularly shaped substrates, such as flat panel displays or machine tools and dies. This is illustrated in Fig. 1.5. Further details are given in Chapter 16.

1.2 PLASMAS AND SHEATHS

Plasmas

A plasma is a collection of free charged particles moving in random directions that is, on the average, electrically neutral (see Fig. 1.6a). This book deals with weakly ionized plasma discharges, which are plasmas having the following features: (1) they are driven electrically; (2) charged particle collisions with neutral gas molecules are important; (3) there are boundaries at which surface losses are important; (4) ionization of neutrals sustains the plasma in the steady state and (5) the electrons are not in thermal equilibrium with the ions. A simple discharge is shown schematically

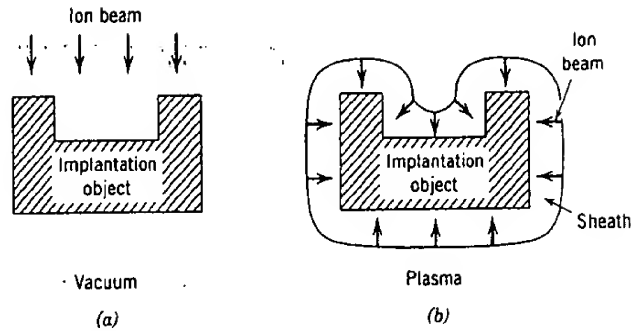

FIGURE 1.5. Illustrating ion implantation of an irregular object: (a) In a conventional ion beam implanter, the beam is electrically scanned and the target object is mechanically rotated and tilted to achieve uniform implantation; (b) in plasma-immersion ion implantation (PIII), the target is immersed in a plasma, and ions from the plasma are implanted with a relatively uniform spatial distribution.

in Fig. 1.6b. It consists of a voltage source that drives current through a low-pressure gas between two parallel conducting plates or electrodes. The gas "breaks down" to form a plasma, usually weakly ionized, i.e., the plasma density is only a small fraction of the neutral gas density. We describe some qualitative features of plasmas in this section; discharges are described in the following section.

Plasmas are often called a fourth state of matter. As we know, a solid substance in thermal equilibrium generally passes into a liquid state as the temperature is increased at a fixed pressure. The liquid passes into a gas as the temperature is further increased. At a sufficiently high temperature, the molecules in the gas decompose to form a gas of atoms that move freely in random directions, except for infrequent collisions between atoms. If the temperature is further increased, then the atoms decompose into freely moving charged particles (electrons and positive ions), and the substance enters the plasma state. This state is characterized by a common charged particle density $n_e \approx n_i \approx n$ particles/m^3 and, in equilibrium, a temperature $T_e = T_i = T$. The temperatures required to form plasmas from pure substances in thermal

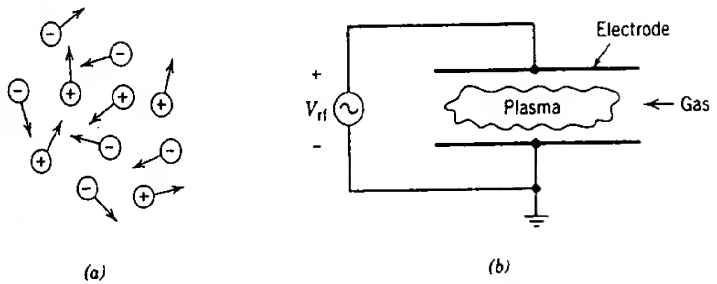

FIGURE 1.6. Schematic view of (a) a plasma and (b) a discharge.

equilibrium range from roughly 4000 K for easy-to-ionize elements like cesium to 20000 K for hard-to-ionize elements like helium. The fractional ionization of a plasma is

$$x_{iz} = \frac{n_i}{n_g + n_i}$$

where n_g is the neutral gas density. x_{iz} is near unity for fully ionized plasmas, and $x_{iz} \ll 1$ for weakly ionized plasmas.

Much of the matter in the universe is in the plasma state. This is true because stars, as well as most interstellar matter, are plasmas. Although stars are plasmas in thermal equilibrium, the light and heavy charged particles in low-pressure processing discharges are *almost never* in thermal equilibrium, either between themselves or with their surroundings. Because these discharges are electrically driven and are weakly ionized, the applied power preferentially heats the mobile electrons, while the heavy ions efficiently exchange energy by collisions with the background gas. Hence, $T_e \gg T_i$ for these plasmas.

Figure 1.7 identifies different kinds of plasmas on a log n versus log T_e diagram. There is an enormous range of densities and temperatures for both laboratory and space plasmas. Two important types of processing discharges are indicated on the figure. Low-pressure discharges are characterized by $T_e \approx 1$–10 V, $T_i \ll T_e$, and $n \approx 10^8$–10^{13} cm^{-3}. These discharges are used as miniature chemical factories in which feedstock gases are broken into positive ions and chemically reactive etchants, deposition precursors, etc., which then flow to and physically or chemically react at the substrate surface. While energy is delivered to the substrate also, e.g., in the form of bombarding ions, the energy flux is there to promote the chemistry at the substrate, and not to heat the substrate. The gas pressures for these discharges are low: $p \approx 1$ mTorr–1 Torr. *These discharges and their use for processing are the principal subject of this book.* We give the quantitative framework for their analysis in Chapter 10.

High-pressure arc discharges are also used for processing. These discharges have $T_e \approx 0.1$–2 V and $n \approx 10^{14}$–10^{19} cm^{-3}, and the light and heavy particles are more nearly in thermal equilibrium, with $T_i \leq T_e$. These discharges are used mainly to deliver heat to the substrate, e.g., to increase surface reaction rates, to melt, sinter, or evaporate materials, or to weld or cut refractory materials. Operating pressures are typically near atmospheric pressure (760 Torr). High-pressure discharges of this type are beyond the scope of this book.

Figure 1.8 shows the densities and temperatures (or average energies) for various species in a typical rf-driven capacitively coupled low-pressure discharge; e.g., for silicon etching using CF_4, as described in Section 1.1. We see that the feedstock gas, etchant atoms, etch product gas, and plasma ions have roughly the same temperature, which does not exceed a few times room temperature (0.026 V). The etchant F and product SiF_4 densities are significant fractions of the CF_4 density, but the fractional ionization is very low: $n_i \sim 10^{-5} n_g$. The electron temperature T_e is two orders of magnitude larger than the ion temperature T_i. However, we note that the energy of ions

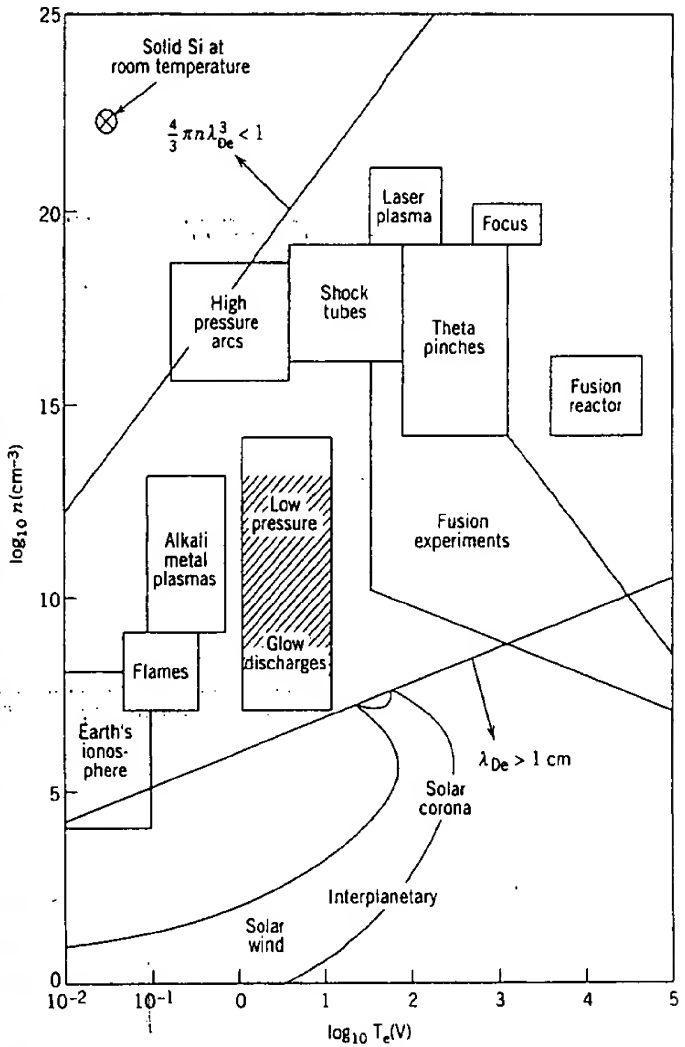

FIGURE 1.7. Space and laboratory plasmas on a log n versus log T_e diagram (after Book, 1987). λ_{De} is defined in Section 2.4.

bombarding the substrate can be 100–1000 V, much exceeding T_e. The acceleration of low-temperature ions across a thin *sheath* region where the plasma and substrate meet is central to all processing discharges. We describe this qualitatively below and quantitatively in later chapters.

Although n_i, n_e may be five orders of magnitude lower that n_g, the charged particles play central roles in sustaining the discharge and in processing. Because $T_e \gg T_i$, it is the electrons that dissociate the feedstock gas to create the free radicals,

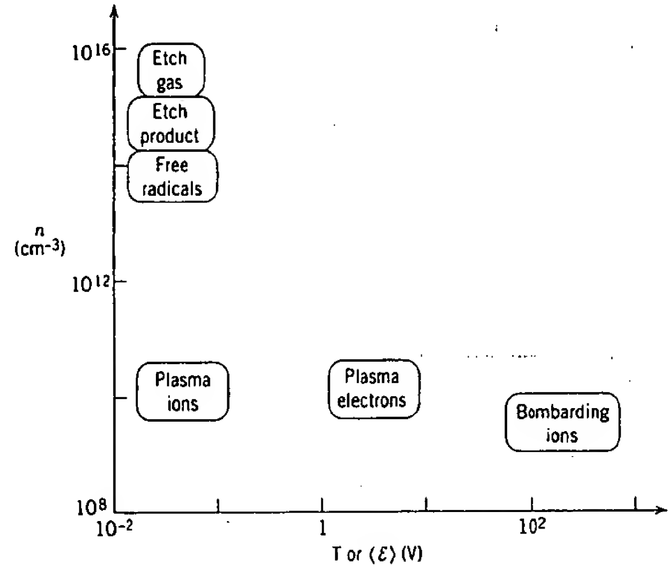

FIGURE 1.8. Densities and energies for various species in a low-pressure capacitive rf discharge.

etchant atoms, and deposition precursors, required for the chemistry at the substrate. Electrons also ionize the gas to create the positive ions that subsequently bombard the substrate. As we have seen, energetic ion bombardment can increase chemical reaction rates at the surface, clear inhibitor films from the surface, and physically sputter materials from or implant ions into the surface.

T_e is generally less than the threshold energies $\mathcal{E}_{diss}$ or $\mathcal{E}_{iz}$ for dissociation and ionization of the feedstock gas molecules. Nevertheless, dissociation and ionization occur because electrons have a distribution of energies. Letting $g_e(\mathcal{E})\,d\mathcal{E}$ be the number of electrons per unit volume with energies lying between $\mathcal{E}$ and $\mathcal{E} + d\mathcal{E}$, then the distribution function $g_e(\mathcal{E})$ is sketched in Fig. 1.9. Electrons having energies below

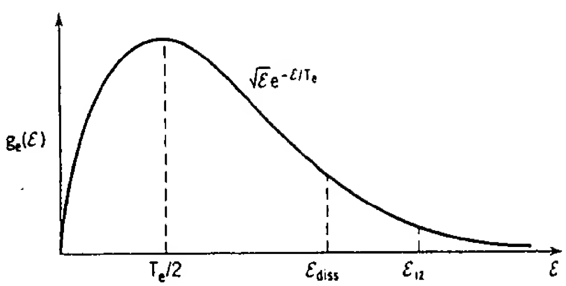

FIGURE 1.9. Electron distribution function in a weakly ionized discharge.

$\mathcal{E}_{diss}$ or $\mathcal{E}_{iz}$ cannot dissociate or ionize the gas. We see that dissociation and ionization are produced by the high-energy tail of the distribution. Although the distribution is sketched in the figure as if it were Maxwellian at the bulk electron temperature T_e, this may not be the case. The tail distribution might be depressed below or enhanced above a Maxwellian by electron heating and electron–neutral collision processes. Two temperature distributions are sometimes observed, with T_e for the bulk electrons lower than T_h for the energetic electron tail.

Sheaths

Plasmas, which are quasineutral ($n_i \approx n_e$), are joined to wall surfaces across thin positively charged layers called *sheaths*. To see why, first note that the electron thermal velocity $(eT_e/m)^{1/2}$ is at least 100 times the ion thermal velocity $(eT_i/M)^{1/2}$ because $m/M \ll 1$ and $T_e \gtrsim T_i$. (Here, T_e and T_i are given in units of volts.) Consider a plasma of width l with $n_e = n_i$ initially confined between two grounded ($\Phi = 0$) absorbing walls (Fig. 1.10a). Because the net charge density $\rho = e(n_i - n_e)$ is zero, the electric potential Φ and the electric field E_x is zero everywhere. Hence, the fast-moving electrons are not confined and will rapidly be lost to the walls. On a very short timescale, however, some electrons near the walls are lost, leading to the situation shown in Fig. 1.10b. Thin ($s \ll l$) positive ion sheaths form near each wall in which $n_i \gg n_e$. The net positive ρ within the sheaths leads to a potential profile $\Phi(x)$ that is positive within the plasma and falls sharply to zero near both walls. This acts as a confining potential "valley" for electrons and a "hill" for ions because the

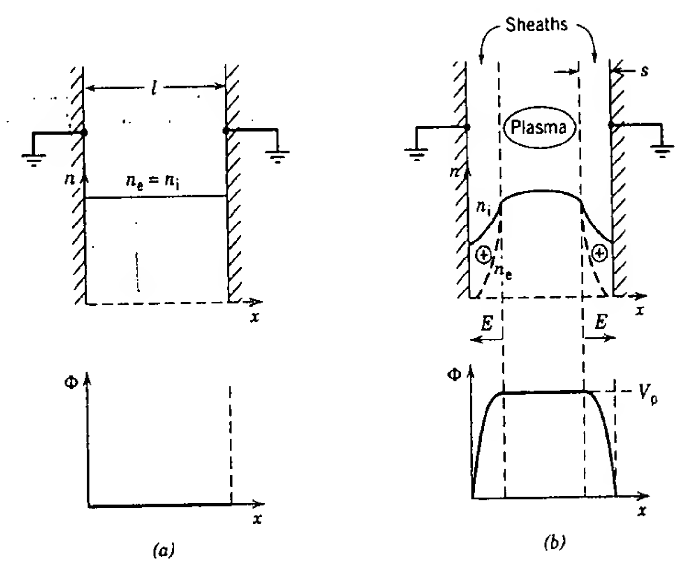

FIGURE 1.10. The formation of plasma sheaths: (a) initial ion and electron densities and potential; (b) densities, electric field, and potential after formation of the sheath.

electric fields within the sheaths point from the plasma to the wall. Thus the force $-eE_x$ acting on electrons is directed into the plasma; this reflects electrons traveling toward the walls back into the plasma. Conversely, ions from the plasma that enter the sheaths are accelerated into the walls. If the plasma potential (with respect to the walls) is V_p, then we expect that $V_p \sim$ a few T_e in order to confine most of the electrons. The energy of ions bombarding the walls is then $\mathcal{E}_i \sim$ a few T_e. Charge uncovering is treated quantitatively in Chapter 2, and sheaths in Chapter 6.

Figure 1.11 shows sheath formation as obtained from a particle-in-cell (PIC) plasma simulation. We use PIC results throughout this book to illustrate various discharge phenomena. In this simulation, the left wall is grounded, the right wall is floating (zero net current), and the positive ion density is uniform and constant in time. The electrons are modeled as $\mathcal{N}$ sheets having charge-to-mass ratio $-e/m$ that move in one dimension (along x) under the action of the time-varying fields produced by all the other sheets, the fixed ion charge density, and the charges on the walls. Electrons do not collide with other electrons, ions, or neutrals in this simulation. Four thousand sheets were used with $T_e = 1$ V and $n_i = n_e = 10^{13}$ m^{-3} at time $t = 0$. In (a), (b), (c), and (d), we see the v_x–x electron phase space, electron density, electric field, and potential after the sheath has formed, at $t = 0.77$ μs. The time history of $\mathcal{N}$ is shown in (e); 40 sheets have been lost to form the sheaths. Figures 1.11a–d show the absence of electrons near each wall over a sheath width $s \approx 6$ mm. Except for fluctuations due to the finite $\mathcal{N}$, the field in the bulk plasma is near zero, and the fields in the sheaths are large and point from the plasma to the walls. (E_x is negative

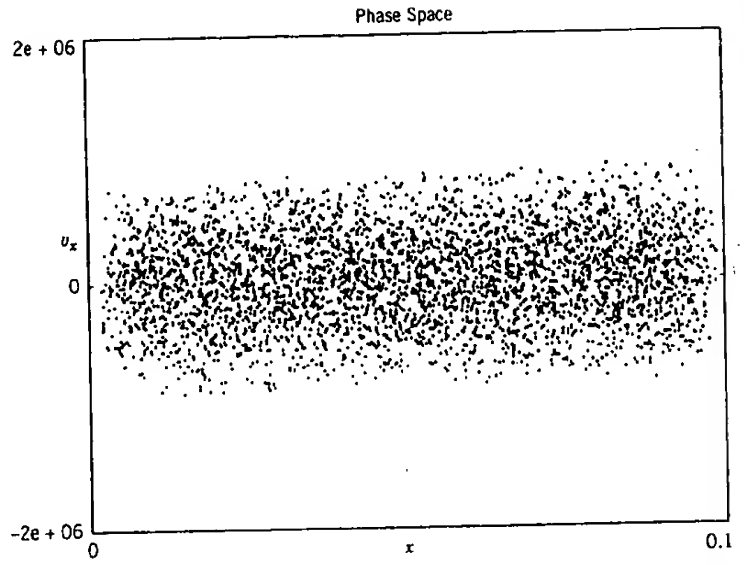

(a)

FIGURE 1.11. PIC simulation of positive ion sheath formation: (a) v_x–x electron phase space, with horizontal scale in meters.

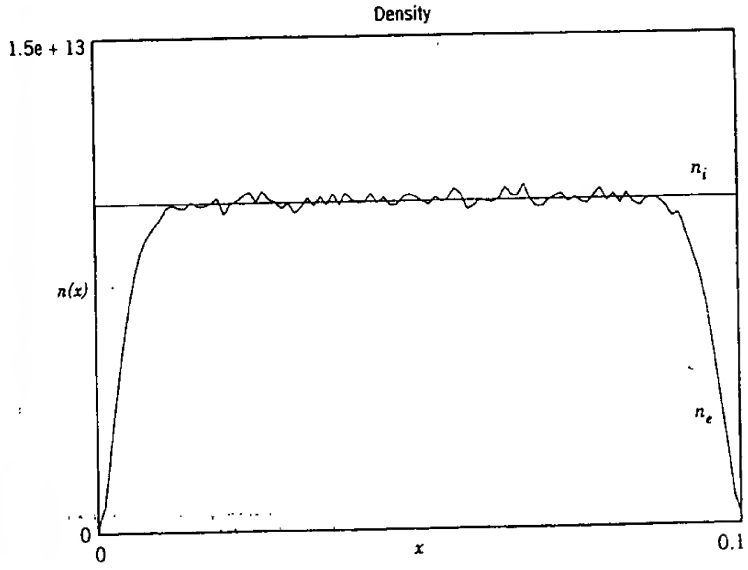

(b)

FIGURE 1.11. (*continued*) PIC simulation of positive ion sheath formation: (b) electron density n_e.

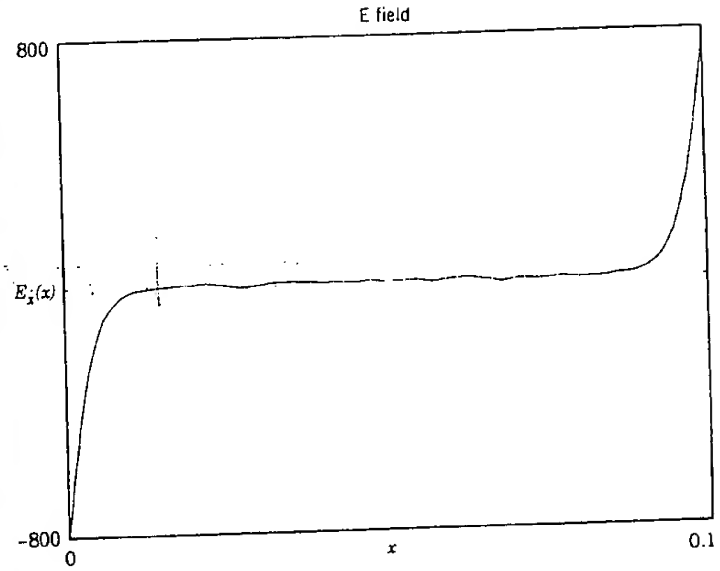

(c)

FIGURE 1.11. (*continued*) PIC simulation of positive ion sheath formation: (c) electric field E_x.

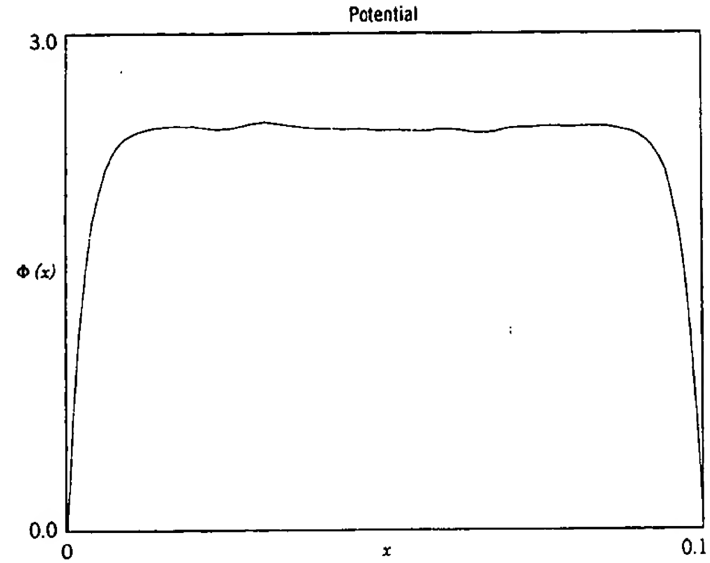

(d)

FIGURE 1.11. *(continued)* PIC simulation of positive ion sheath fomation: (d) potential Φ.

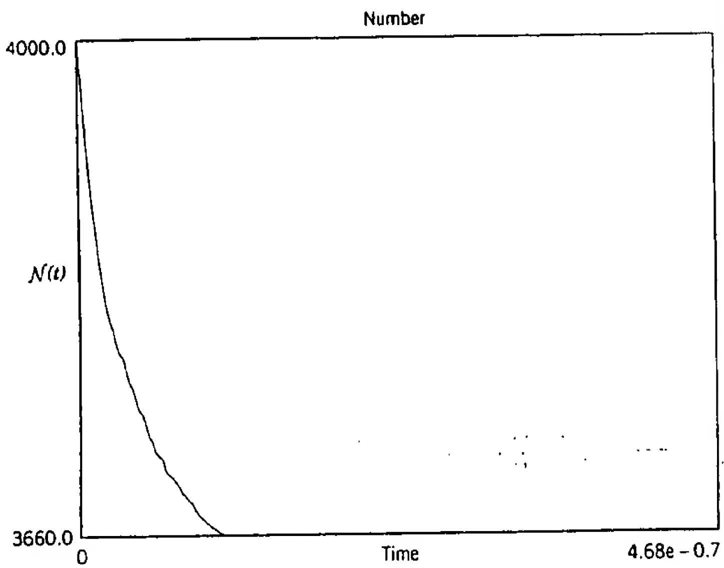

(e)

FIGURE 1.11. *(continued)* PIC simulation of positive ion sheath formation: (e) electron number $\mathcal{N}$ versus time t in seconds.

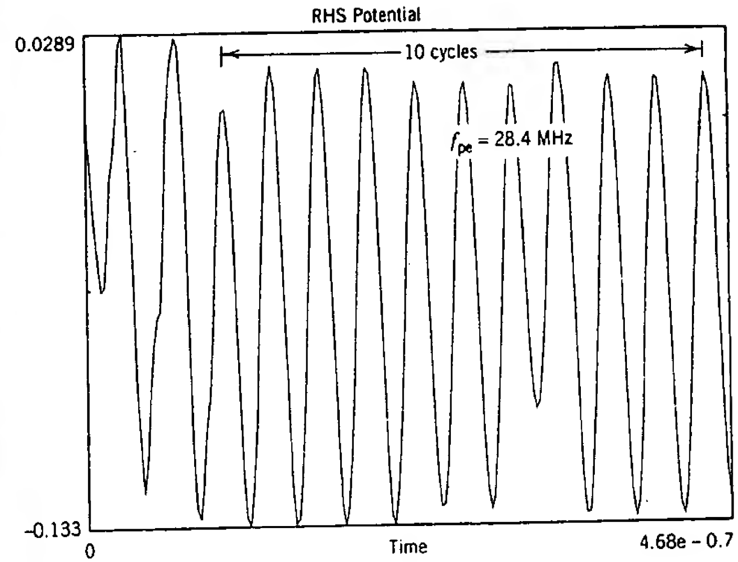

(f)

FIGURE 1.11. *(continued)* PIC simulation of positive ion sheath formation: (f) right hand potential V_r versus time t.

at the left wall and positive at the right wall to repel plasma electrons.) The potential in the center of the discharge is $V_p \approx 2.5$ V and falls to zero at the left wall (this wall is grounded by definition). The potential at the right wall is also low, but we see in (f) that it oscillates in time. We will see in Chapter 4 that these are *plasma oscillations*. We would not see them if the initial sheet positions and velocities were chosen exactly symmetrically about the midplane, or if many more sheets were used in the simulation.

If the ions were also modeled as moving sheets, then on a longer time scale we would see ion acceleration within the sheaths, and a consequent drop in ion density near the walls, as sketched in Fig. 1.10b. We return to this in Chapter 6.

The separation of discharges into bulk plasma and sheath regions is an important paradigm that applies to all discharges. The bulk region is quasineutral, and both instantaneous and time-averaged fields are low. The bulk plasma dynamics are described by diffusive ion loss at high pressures and by free-fall ion loss at low pressures. In the positive space charge sheaths, high fields exist, leading to dynamics that are described by various ion space charge sheath laws, including low-voltage sheaths and various high-voltage sheath models, such as collisionless and collisional Child laws and their modifications. The plasma and sheath dynamics must be joined at their interface. As will be seen in Chapter 6, the usual joining condition is to require that the mean ion velocity at the plasma-sheath edge be equal to the ion-sound (Bohm) velocity: $u_B = (e\mathrm{T}_e/M)^{1/2}$, where e and M are the charge and mass of the ion and T_e is the electron temperature in volts.

1.3 DISCHARGES

Rf Diodes

Capacitively driven radio frequency (rf) discharges—so-called *rf diodes*—are commonly used for materials processing. An idealized discharge in plane parallel geometry, shown in Fig. 1.12a, consists of a vacuum chamber containing two planar electrodes separated by a spacing l and driven by an rf power source. The substrates are placed on one electrode, feedstock gases are admitted to flow through the discharge, and effluent gases are removed by the vacuum pump. Coaxial discharge geometries, such as the "hexode" shown in Fig. 1.12b, are also in widespread use. Typical parameters are shown in Table 1.1. The typical rf driving voltage is V_{rf} = 100–1000 V, and the plate separation is l = 2–10 cm. When operated at low pressure, with the wafer mounted on the powered electrode, and used to remove substrate material, such reactors are commonly called reactive ion etchers (RIEs)—a misnomer, since the etching is a chemical process enhanced by energetic ion bombardment of the substrate, rather than a removal process due to reactive ions alone.

For anisotropic etching, typically pressures are in the range 10–100 mTorr, power densities are 0.1–1 W/cm^2, the driving frequency is 13.56 MHz, and multiple wafer systems are common. Typical plasma densities are relatively low, 10^9–10^{11} cm^{-3}, and the electron temperature is of order 3 V. Ion acceleration energies (sheath voltages) are high, greater than 200 V, and fractional ionization is low. The degree of dissociation of the molecules into reactive species is seldom measured but can range widely from less than 0.1% to nearly 100% depending on gas composition and plasma conditions. For deposition and isotropic etch applications, pressures tend to be higher, ion bombarding energies are lower, and frequencies can be lower than the commonly used standard of 13.56 MHz.

The operation of capacitively driven discharges is reasonably well understood. As shown in Fig. 1.13 for a symmetrically driven discharge, the mobile plasma electrons, responding to the instantaneous electric fields produced by the rf driving voltage, oscillate back and forth within the positive space charge cloud of the ions. The massive ions respond only to the time-averaged electric fields. Oscillation of the electron cloud creates sheath regions near each electrode that contain net positive

TABLE 1.1. Range of Parameters for Rf Diode and High-Density Discharges

Parameter	Rf Diode	High-Density Source
Pressure p (m Torr)	10–1000	0.5–50
Power P (W)	50–2000	100–5000
Frequency f (MHz)	0.05–13.56	0–2450
Volume $\mathcal{V}$ (L)	1–10	2–50
Cross-sectional area A (cm^2)	300–2000	300–500
Magnetic field B (kG)	0	0–1
Plasma density n (cm^{-3})	10^9–10^{11}	10^{10}–10^{12}
Electron temperature T_e (V)	1–5	2–7
Ion acceleration energy $\mathcal{E}_i$ (V)	200–1000	20–500
Fractional ionization x_{i2}	10^{-6}–10^{-3}	10^{-4}–10^{-1}

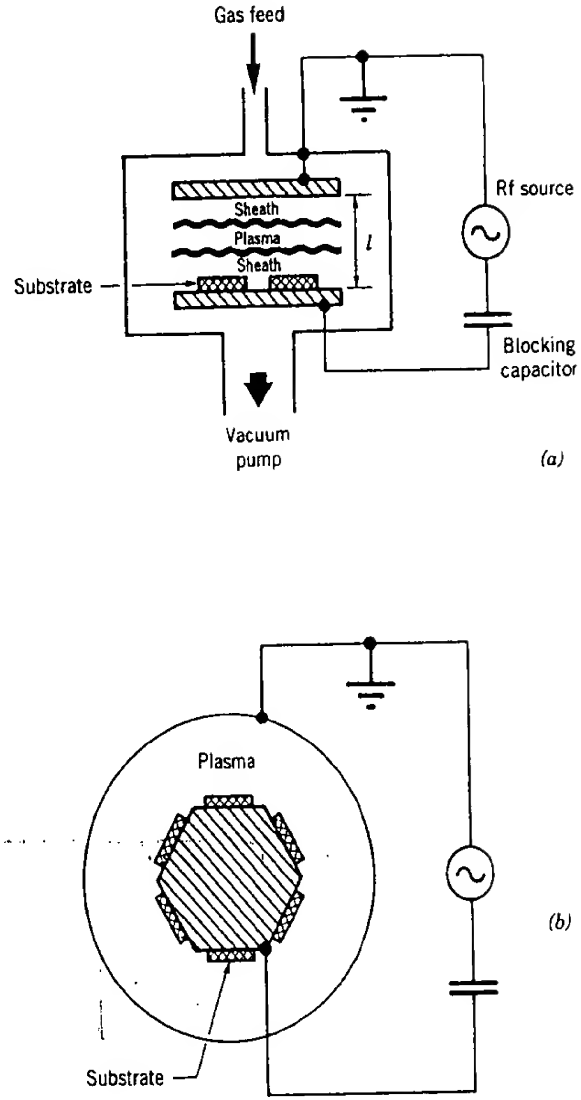

FIGURE 1.12. Capacitive rf discharges in (a) plane parallel geometry and (b) coaxial "hexode" geometry. (From "Design of High-Density Sources for Materials Processing" from the work "Physics of Thin Films," Vol. 18, by Academic Press, Inc., Publisher in Press)

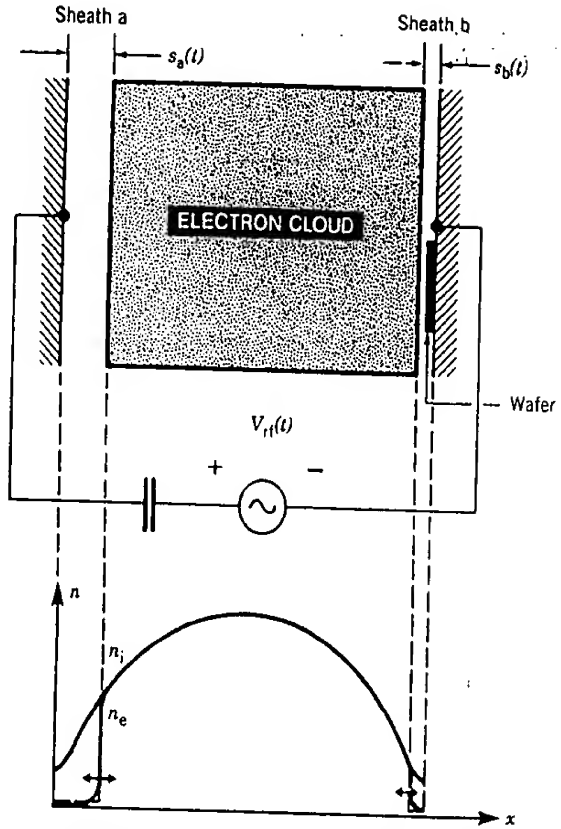

FIGURE 1.13. The physical model of an rf diode. (From "Design of High-Density Sources for Materials Processing" from the work "Physics of Thin Films," Vol. 18, by Academic Press, Inc., Publisher in Press)

charge when averaged over an oscillation period; i.e., the positive charge exceeds the negative charge in the system, with the excess appearing within the sheaths. This excess produces a strong time-averaged electric field within each sheath directed from the plasma to the electrode. Ions flowing out of the bulk plasma near the center of the discharge can be accelerated by the sheath fields to high energies as they flow to the substrate, leading to energetic-ion enhanced processes. Typical ion-bombarding energies $\mathcal{E}_i$ can be as high as $V_{rf}/2$ for symmetric systems (Fig. 1.13) and as high as V_{rf} at the powered electrode for asymmetric systems (Fig. 1.12). A quantitative description of capacitive discharges is given in Chapter 11.

We note that the positive ions continuously bombard the electrode over an rf cycle. In contrast, electrons are lost to the electrode only when the oscillating cloud closely approaches the electrode. During that time, the instantaneous sheath potential collapses to near zero, allowing sufficient electrons to escape to balance the ion charge delivered to the electrode. Except for such brief moments, the instantaneous potential of the discharge must always be positive with respect to any large electrode and wall surface; otherwise the mobile electrons would quickly leak out. Electron confinement is ensured by the presence of positive space charge sheaths near all surfaces.

We will see that a crucial limiting feature of rf diodes is that the ion-bombarding flux $\Gamma_i = nu_B$ and bombarding energy $\mathcal{E}_i$ cannot be varied independently. The situation is analogous to the lack of independent voltage and current control in diode vacuum tubes or semiconductor pn junctions. For a reasonable (but relatively low) ion flux, as well as a reasonable dissociation of the feedstock gas, sheath voltages at the driven electrode are high. For wafers placed on the driven electrode, this can result in undesirable damage, or loss of linewidth control. Furthermore, the combination of low ion flux and high ion energy leads to a relatively narrow process window for many applications. The low process rates resulting from the limited ion flux in rf diodes often mandates multiwafer or batch processing, with consequent loss of wafer-to-wafer reproducibility. Higher ion and neutral fluxes are generally required for single-wafer processing in a clustered tool environment, in which a single wafer is moved by a robot through a series of process chambers. Clustered tools are used to control interface quality and are said to have the potential for significant cost savings in fabricating integrated circuits. Finally, low fractional ionization poses a significant problem for processes where the feedstock costs and disposal of effluents are issues.

To meet the linewidth, selectivity, and damage control demands for next-generation fabrication, the mean ion bombarding energy, and its energy distribution, should be controllable independently of the ion and neutral fluxes. Some control over ion-bombarding energy can be achieved by putting the wafer on the undriven electrode and independently biasing this electrode with a second rf source. Although these so-called *rf triode* systems are in use, processing rates are still low at low pressures and sputtering contamination is an issue.

Various magnetically enhanced rf diodes and triodes have also been developed to improve performance of the rf reactor. These include, for example, magnetically enhanced reactive ion etchers (MERIEs), in which a dc magnetic field of 50–300 G is applied parallel to the powered electrode, on which the wafer sits. The magnetic field increases the efficiency of power transfer from the source to the plasma and also enhances plasma confinement. This results in a reduced sheath voltage and an increased plasma density when the magnetic field is applied. However, the plasma generated is strongly nonuniform both radially and azimuthally. To increase process uniformity (at least azimuthally), the magnetic field is slowly rotated in the plane of the wafer, e.g., at a frequency of 0.5 Hz. While this is an improvement, MERIE systems may not have good uniformity, which may limit their applicability to next-generation, submicrometer device fabrication.

High-Density Sources

The limitations of rf diodes and their magnetically enhanced variants have led to the development of a new generation of low-pressure, high-density plasma sources. A few examples are shown schematically in Fig. 1.14, and typical source and plasma parameters are given in Table 1.1. A quantitative description is given in Chapters 12

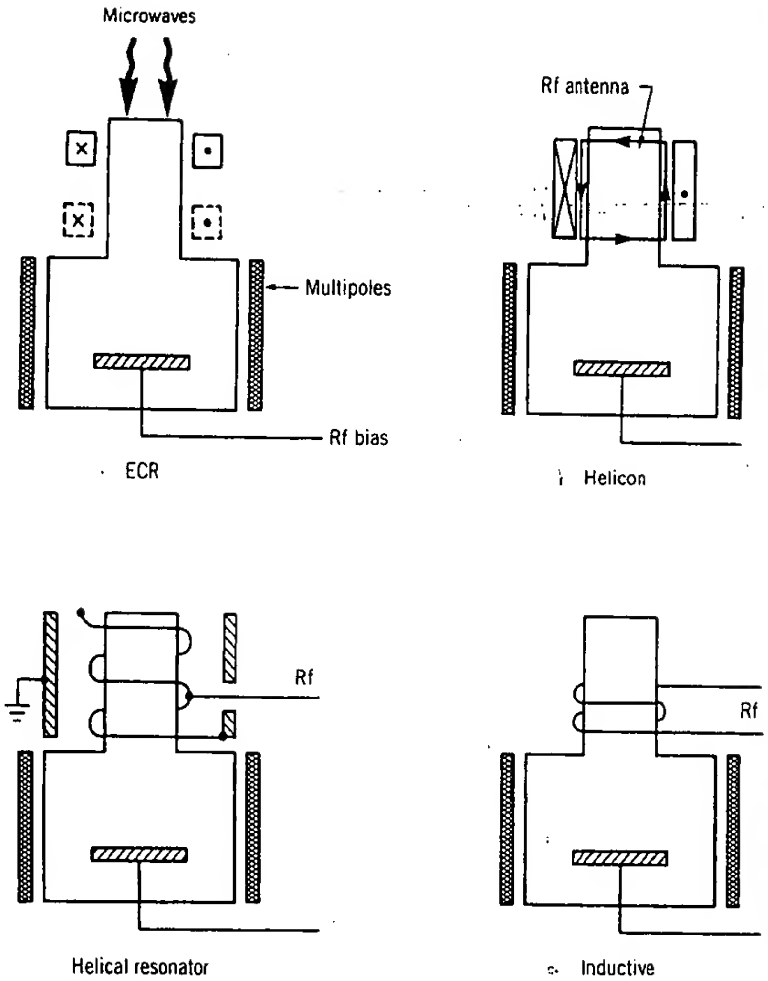

FIGURE 1.14. Some high-density "remote" sources. (From "Design of High-Density Sources for Materials Processing" from the work "Physics of Thin Films," Vol. 18, by Academic Press, Inc., Publisher in Press)

and 13. In addition to high density and low pressure, a common feature is that the rf or microwave power is coupled to the plasma across a dielectric window, rather than by direct connection to an electrode in the plasma, as for an rf diode. This noncapacitive power transfer is the key to achieving low voltages across all plasma sheaths at electrode and wall surfaces. Dc voltages, and hence ion acceleration energies, are then typically 20–30 V at all surfaces. To control the ion energy, the electrode on which the wafer is placed can be independently driven by a capacitively coupled rf source. Hence independent control of the ion/radical fluxes (through the source power) and the ion-bombarding energy (through the wafer electrode power) is possible.

The common features of power transfer across dielectric windows and separate bias supply at the wafer electrode are illustrated in Fig. 1.14. However, sources differ significantly in the means by which power is coupled to the plasma. For the electron cyclotron resonance (ECR) source shown in Fig. 1.14a, one or more electromagnet coils surrounding the cylindrical source chamber generate an axially varying dc magnetic field. Microwave power is injected axially through a dielectric window into the source plasma, where it excites a right-hand circularly polarized wave that propagates to a resonance zone, for cold electrons at $\omega = \omega_{ce}$, where the wave is absorbed. Here $\omega = 2\pi f$ is the applied radian frequency and $\omega_{ce} = eB/m$ is the electron gyration frequency at resonance. For the typical microwave frequency used, $f = 2450$ MHz, the resonant magnetic field is $B \approx 875$ G. The plasma streams out of the source into the process chamber in which the wafer is located.

A helicon source is shown in Fig. 1.14b. A weak (50–200 G) dc axial magnetic field together with an rf-driven antenna placed around the dielectric cylinder that forms the source chamber allows excitation of a helicon wave within the source plasma. Resonant wave–particle interaction is believed to transfer the wave energy to the plasma. For the helical resonator source shown in Fig. 1.14c, the external helix and conducting cylinder surrounding the dielectric discharge chamber form a slow wave structure, i.e., supporting an electromagnetic wave with phase velocity much less than the velocity of light. Efficient coupling of the rf power to the plasma is achieved by excitation of a resonant axial mode. An inductive (or transformer) coupled source is shown in Fig. 1.14d. Here the plasma acts as a single-turn, lossy conductor that is coupled to a multiturn nonresonant rf coil across the dielectric discharge chamber; rf power is inductively coupled to the plasma by transformer action. In contrast to ECR and helicon sources, a dc magnetic field is not required for efficient power coupling in helical resonator or inductive sources.

Figure 1.14 also illustrates the use of high-density sources to feed plasma into a relatively distinct, separate process chamber in which the wafer is located. As shown in the figure, the process chamber can be surrounded by dc multipole magnetic fields to enhance plasma confinement near the process chamber surfaces, while providing a magnetic near-field-free plasma environment at the wafer. Such configurations are often called "remote" sources, a misnomer since at low pressures considerable plasma and free radical production occurs within the process chamber near the wafer. Sometimes, the source and process chambers are more integral, e.g., the wafer is placed very near to the source exit, to obtain increased ion and radical fluxes, reduced spread in ion energy, and improved process uniformity. But the wafer is then exposed to higher levels of damaging radiation.

Although the need for low pressures, high fluxes, and controllable ion energies has motivated high-density source development, there are many issues that need to be resolved. A critical issue is achieving the required process uniformity over 200– to 300–mm wafer diameters. In contrast to the nearly one-dimensional geometry of typical rf diodes (two closely spaced parallel electrodes), high-density cylindrical sources can have length-to-diameter ratios of order or exceeding unity. Plasma formation and transport in such geometries are inherently radially nonuniform. Another critical issue is efficient power transfer (coupling) across dielectric windows over a

wide operating range of plasma parameters. Degradation of and deposition on the window can also lead to irreproducible source behavior and the need for frequent, costly cleaning cycles. Low-pressure operation leads to severe pumping requirements for high deposition or etching rates and hence to the need for large, expensive vacuum pumps. Furthermore, plasma and radical concentrations become strongly sensitive to reactor surface conditions, leading to problems of reactor aging and process irreproducibility. Finally, dc magnetic fields are required for some source concepts. These can lead to magnetic field-induced process nonuniformities and damage, as seen, for example, in MERIE systems.

Figure 1.15 illustrates schematically the central problem of discharge analysis, using the example of an rf diode. Given the *control* parameters for the power source (frequency ω, driving voltage V_{rf} or absorbed power P_{abs}), the feedstock gas (pressure p, flow rate, and chemical composition), and the geometry (simplified here to the discharge length l), then find the *plasma* parameters, including the plasma density n_i, the etchant density n_F, the ion and etchant fluxes Γ_i and Γ_F hitting the substrate, the electron and ion temperatures T_e and T_i, the ion bombarding energy $\mathcal{E}_i$, and the sheath thickness s. The control parameters are the "knobs" that can be "turned" in order to "tune" the properties of the discharge.

The tuning range for a given discharge is generally limited. Sometimes one type of discharge will not do the job no matter how it is tuned, so another type must be selected. As suggested in Figs. 1.12 and 1.14, a bewildering variety of discharges are used for processing. Some are driven by rf, some by dc, and some by microwave power sources. Some use magnetic fields to increase the plasma confinement or the efficiency of power absorption. One purpose of this book is to guide the reader toward making wise choices when designing discharges used for processing.

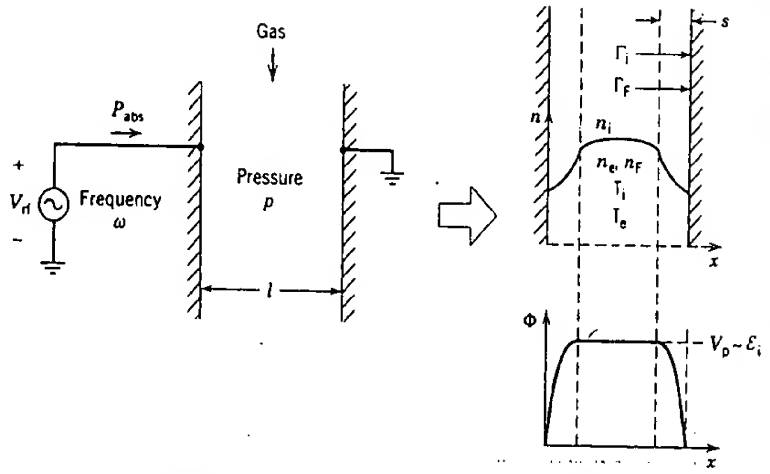

FIGURE 1.15. The central problem of discharge analysis.

1.4 SYMBOLS AND UNITS

The choice of symbols is always vexing. While various fields each have their consistent set of symbols to represent physical quantities, these overlap between different fields, e.g., plasma physics and gas-phase chemistry. For example, H is standard for enthalpy in chemistry but is also standard for magnetic field in plasma physics. This also occurs within a given field; e.g., k is standard for Boltzmann's constant but also for wave number. Then there is always the occasional symbol that must stand for many things in different contexts. We sometimes distinguish these by using different lettering (Roman, italic, script, boldface); e.g., I is a current and I is a modified Bessel function; M is an ion mass and $\mathcal{M}$ is the number of chemical species. We can often distinguish commonly used symbols by the use of subscripts; e.g., σ denotes a cross section, but σ_{rf} and σ_{dc} denote electrical conductivities; we have done this whenever the notation is not too cumbersome. The meaning should be clear from the context, in most cases. To help avoid confusion, we have provided a table of symbols and abbreviations in the front matter of this book. These give the normal usage of symbols and their units.

As far as possible, we use the SI (MKS) system of units: meters (m), kilograms (kg), seconds (s), and coulombs (C) for charge. In these units, the charge on an electron is $-e \approx -1.602 \times 10^{-19}$ C. The unit of energy is the joule (J), but we often use the symbol $\mathcal{E}$ for the voltage that is the equivalent of the energy; i.e.,

$$U(\text{joules}) = e\mathcal{E}$$

where $\mathcal{E}$ is in volts. We also occasionally use the calorie (cal): 1 cal $\approx$ 4.187 J. The SI unit of pressure is the pascal (Pa), but we more commonly give gas pressures in Torr:

$$1 \text{ Torr} \approx 133.3 \text{ Pa}$$

We occasionally use 1 atm $\approx 1.013 \times 10^5$ Pa $\approx$ 760 Torr and 1 bar $= 10^5$ Pa to refer to gas pressures. The SI unit for the magnetic induction B is tesla (T), but we more often give B in gauss (G): 1 T $= 10^4$ G. We use the symbol T to refer to the temperature in kelvins (K). The energy equivalent temperature in joules is kT, where $k \approx 1.381 \times 10^{-23}$ J/K is Boltzmann's constant. We often use the roman typeface symbol T for the voltage equivalent of the temperature, where

$$e\mathrm{T}(\text{volts}) = kT(\text{kelvins})$$

Hence room temperature $T = 297$ K is equivalent to T $\approx$ 0.026 V. Even within the standard unit system, quantities are often designated by subunits. For example, cross sections are often given in cm^2 rather than m^2 in tables, and wavelengths at microwave frequencies are commonly given in cm rather than in meters.

To assist our readers in making calculations, we give the commonly used constants in the SI system of units and the most common conversions between units in the front matter of the book. It is sometimes tempting to make a calculation in nonstandard units. For example, the collision frequency $\nu = n\sigma v$, which has units $(m^{-3} \cdot m^2 \cdot m\,s^{-1})$, could equally well be calculated in the commonly used units $(cm^{-3} \cdot cm^2 \cdot cm\,s^{-1})$, since the length units cancel. However, we urge the student not to take such shortcuts, but to systematically convert to standard units, before making a calculation.

CHAPTER 2

BASIC PLASMA EQUATIONS AND EQUILIBRIUM

2.1 INTRODUCTION

The plasma medium is complicated in that the charged particles are both affected by external electric and magnetic fields and contribute to them. The resulting self-consistent system is nonlinear and very difficult to analyze. Furthermore, the interparticle collisions, although also electromagnetic in character, occur on space and time scales that are usually much shorter than those of the applied fields or the fields due to the average motion of the particles.

To make progress with such a complicated system, various simplifying approximations are needed. The interparticle collisions are considered independently of the larger scale fields to determine an *equilibrium distribution* of the charged-particle velocities. The velocity distribution is averaged over velocities to obtain the *macroscopic motion*. The macroscopic motion takes place in external applied fields and in the macroscopic fields generated by the average particle motion. These self-consistent fields are nonlinear, but may be linearized in some situations, particularly when dealing with waves in plasmas. The effect of spatial variation of the distribution function leads to pressure forces in the macroscopic equations. The collisions manifest themselves in particle generation and loss processes, as an average friction force between different particle species, and in energy exchanges among species. In this chapter we consider the basic equations that govern the plasma medium, concentrating attention on the macroscopic system. The complete derivation of these equations, from

(b) Show by integrating the equation above (2.4.10) that the average one-way particle flux is $\Gamma_e = n_e \bar{v}_e/4$.

(c) Find the average one-way energy flux S_e by integrating the energy flux over a Maxwellian distribution. Comparing S_e to Γ_e, show that (2.4.11) holds, i.e., the average kinetic energy per particle crossing a surface is $W_e = 2kT_e$.

2.6. Debye Length A conducting sphere of radius a is immersed in an infinite uniform plasma having density n_0, electrons in thermal equilibrium at temperature T_e, and ions in thermal equilibrium at temperature T_i. A small dc voltage $V_0 \ll T_e, T_i$ is applied to the sphere.

(a) Starting from Poisson's equation in spherical coordinates and using Boltzmann's relation for both the electrons at temperature T_e and the positively charged ions at temperature T_i, derive an expression for the potential $\Phi(r)$ everywhere in the plasma.

(b) Find an expression for the Debye length, and show that the Debye length is determined mainly by the temperature of the colder species.

Hints: Note that for spherical symmetry, $\nabla^2\Phi = (1/r)d^2(r\Phi)/dr^2$. Also note that in a typical discharge, the ions are not in thermal equilibrium. Thus, even though $T_i \ll T_e$ in a discharge, the effective Debye length is usually determined by the electrons alone.

CHAPTER 3

ATOMIC COLLISIONS

3.1 BASIC CONCEPTS

When two particles collide, various phenomena may occur. As examples, one or both particles may change their momentum or their energy, neutral particles can become ionized, and ionized particles can become neutral. We introduce the fundamentals of collisions between electrons, positive ions, and gas atoms in this chapter, concentrating on simple classical estimates of the important processes in noble gas discharges such as argon. For electrons colliding with atoms, the main processes are elastic scattering in which primarily the electron momentum is changed, and inelastic processes such as excitation and ionization. For ions colliding with atoms, the main processes are elastic scattering in which momentum and energy are exchanged, and resonant charge transfer. Other important processes occur in molecular gases. These include dissociation, dissociative recombination, processes involving negative ions, such as attachment, detachment, and positive–negative ion charge transfer, and processes involving excitation of molecular vibrations and rotations. We defer consideration of collisions in molecular gases to Chapter 8.

Elastic and Inelastic Collisions

Collisions conserve momentum and energy: the total momentum and energy of the colliding particles after collision are equal to that before collision. Electrons